MJO-like systems and moisture-convection feedback in idealized aquaplanet simulations

Wojciech W. Grabowski

National Center for Atmospheric Research
Boulder, Colorado, USA.

This paper concerns large-scale organization of tropical convection in general, and Madden-Julian Oscillation (MJO) in particular. Several mechanisms were proposed in the past to explain the large-scale organization, such as coupling of convection with large-scale equatorially-trapped disturbances (e.g., waves); impact of clouds and moisture on radiative transfer; impact of environmental humidity on convective dynamics; impact of convectively-generated gravity waves on subsequent convective development; and atmosphere-ocean interactions (see a discussion and references in Grabowski 2003, hereafter G03). Except for the atmosphere-ocean interactions, the above mechanisms involve only atmospheric processes. The issue of whether MJO involves atmospheric dynamics only or coupled atmosphere-ocean dynamics has recently attracted considerable attention. One has to distinguish, however, between MJO observed in the tropics from MJO-like systems simulated in idealized frameworks (e.g., aquaplanets) where the sea surface temperature (SST) is prescribed.

There is no doubt that the atmosphere-ocean interactions are an integral part of the observed MJO (cf., Lin and Johnson 1996). However, as illustrated by prescribed-SST simulations discussed in G03, the impact of atmospheric processes on the SST and SST feedback on MJO are likely of secondary importance as far as the dynamics of the MJO-like systems are concerned. We would argue that the fact that the MJO is improved in climate simulations using coupled General Circulation Models (GCMs) points to weaknesses in the representation of atmospheric processes in general, and moist convection in particular. On intraseasonal time scales, these weaknesses can be obscured, and possibly remedied, by atmosphere-ocean interactions. Numerical results discussed in this paper illustrate this very point.

G03 investigated MJO-like systems on a rotating constant-SST ("tropics everywhere") aquaplanet using cloud-resolving convection parameterization (CRCP, the super-parameterization; Grabowski 2001). The cornerstone of CRCP is applying a 2D cloud-resolving model in each column of a large-scale model to represent small-scale and mesoscale processes, and couplings among them. The cloud-resolving model replaces a traditional parameterization of convective processes. The aquaplanet considered in G03 has the same size and rate of rotation as Earth and the atmosphere is assumed to be initially at rest. In these simulations, no large-scale organization of convection is present outside the equatorial waveguide. Inside the waveguide, on the other hand, the model simulates spontaneous formation of coherent structures with deep convection on the leading edge and strong surface westerly winds to the west, the westerly wind bursts. These coherent structures resemble MJO observed in the tropics. Figure 1 illustrates the MJO-like system that develops in the second half of the simulation applying prescribed radiative cooling. Similar MJO-like systems develop in simulations applying interactive radiation and increased horizontal resolution of the global model. Sensitivity simulations discussed in G03 demonstrate that the coupling among deep convection, free-tropospheric moisture, and the large-scale flow --- the moisture-convection feedback --- is essential for coherence of the MJO-like systems. When large-scale fluctuations of convectively-generated free-tropospheric moisture are removed on a time scale of a few hours [see (1) in G03], the MJO-like systems do not develop (cf. Fig. 11 in G03) and, if already present, disintegrate rapidly (cf. Figs. 12-15 in G03).

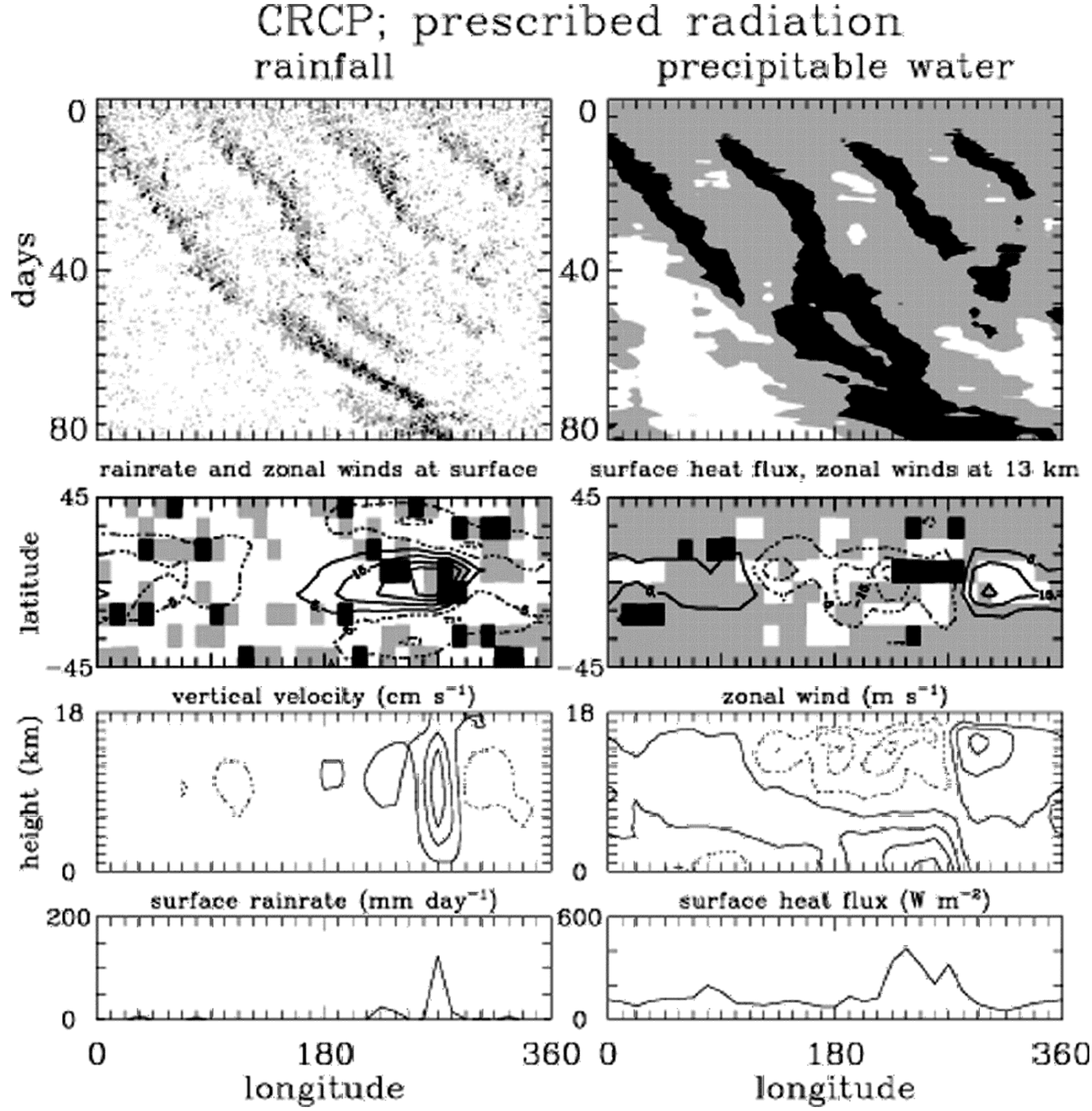

Figure 1. Results from the constant-SST aquaplanet simulation using CRCP. Upper panels show Hovmöller diagrams of the surface precipitation (upper left) and precipitable water (upper right) at the equator. Precipitation intensities larger than 0.2 and 5 mm hr^{-1} are shown using gray and black shading, respectively. Precipitable water smaller/larger than 65/75 kg m^{-2} is shown as white/black; gray shading is for precipitable water between 65 and 75 kg m^{-2}. The second two panels from the top show spatial distribution of surface precipitation and surface zonal winds (left), surface total heat flux (sensible plus latent), and zonal winds at 13 km (right), all at day 80. Precipitation rate (surface heat flux) larger than 1.5 and 15 mm day^{-1} (100 and 250 W m^{-2}) is shown using light and dark shading, respectively. Zonal winds are shown using solid and dashed contours for positive and negative values, respectively, with contour interval of 10 ms^{-1} starting from 5 ms^{-1}. The third row of panels shows vertical (left) and horizontal (right) velocities in the vertical plane at the equator at day 80. Contour interval is 2 cm s^{-1} (10 m s^{-1}) for vertical (horizontal) velocities starting at 1 cm s^{-1} (5 m s^{-1}); solid (dashed) contours are for positive (negative) values. The bottom two panels show spatial distribution of the surface precipitation (left) and the sum of surface sensible and latent heat fluxes (right) along the equator, also at day 80.

Free-tropospheric humidity has long been recognized as an important factor modulating moist convection. A spectacular example is the so-called dry intrusion, where advection of dry subtropical air suppresses tropical convection for a period of about 10 days (see Redelsperger et al. 2002 and references therein). Moisture conditioning of the tropical environment by convective detrainment has long been observed (e.g. Yanai et al.

1973). Convection moistens its immediate environment rendering it more favorable for further convection. The moistening occurs through both convective detrainment and the evaporation of precipitation. Tompkins (2001) postulated that the moisture-convection feedback mechanism is the key in coupling between deep convection and SST fluctuations in the tropics.

Figure 2 illustrates the concept of moisture-convection feedback. The upper panel shows the convective-radiative quasi-equilibrium state. Convective clouds develop randomly in space and time, and maintain horizontally quasi-homogeneous temperature and moisture profiles. The cloud-scale temperature and moisture perturbations disperse through gravity waves and horizontal advection, respectively, on time scales of a few hours. The quasi-equilibrium concept implies that the mean radiative cooling is balanced by the large-scale subsidence warming, with the subsidence being distributed more or less homogeneously between convective clouds and organized cloud systems.

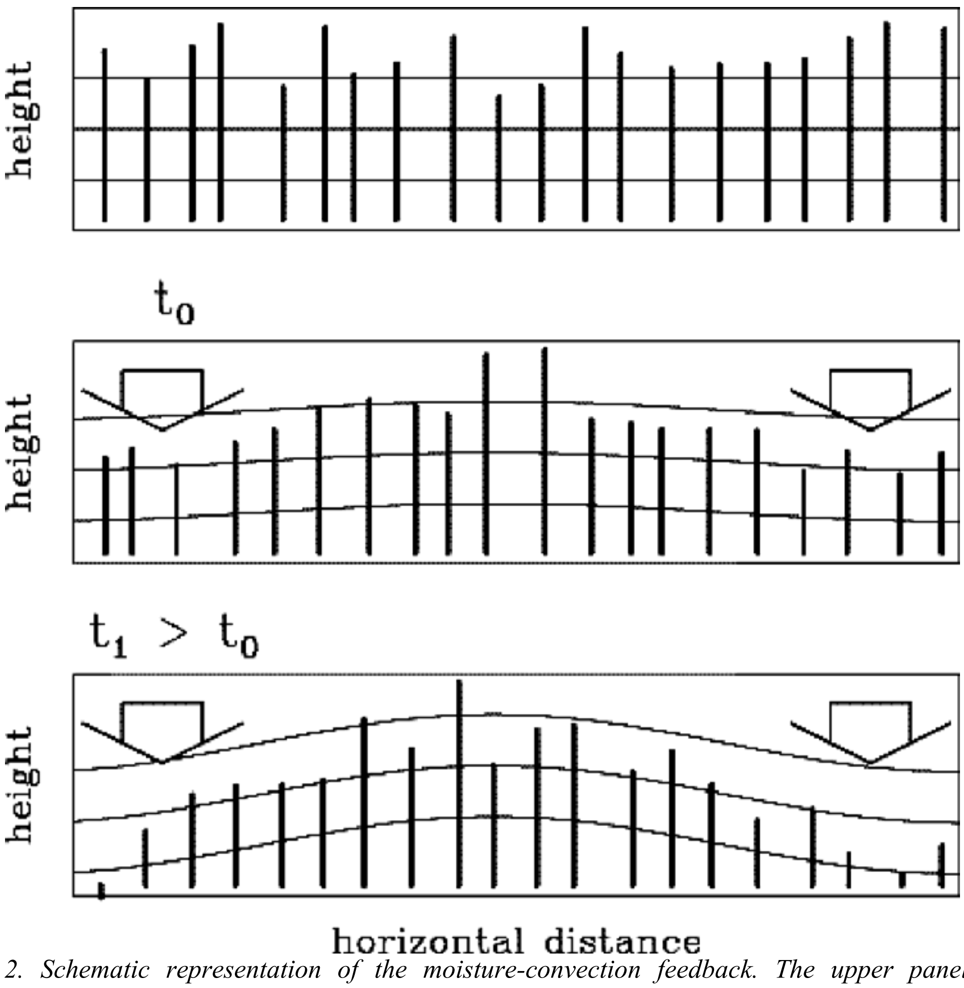

Figure 2. Schematic representation of the moisture-convection feedback. The upper panel shows convective-radiative quasi-equilibrium with horizontal lines representing contours of water vapor mixing ratio and vertical thick lines representing convective clouds at different stages of their development. The middle panel shows the situation shortly after positive large-scale moisture perturbation is added in the center of the domain. The bottom panel shows the situation at a later time. See text for a discussion.

The middle panel shows a hypothetical situation where a positive moisture perturbation is introduced in the free troposphere in the center of the domain. This has two notable effects. First, the entrainment of humid environmental air into convective clouds slows the loss of positive buoyancy compared to the scenario whereby drier environmental air gets entrained. Consequently, a larger proportion of clouds reach the upper troposphere in the center of the domain as schematically illustrated. Second, precipitation falling outside clouds evaporates less when the environmental humidity is enhanced. These two effects strengthen convective heating in the moister environment compared to the drier part of the domain.

In convective-radiative quasi-equilibrium, differences in convective heating must be balanced by the temperature tendency due to the large-scale circulation (especially vertical advection). Locally, their sum must balance the radiative cooling. Therefore an enhanced large-scale subsidence (illustrated by thick arrows remote from the center of the domain) develops in the area with suppressed convection. As time progresses (bottom panel), the large-scale gradient of free-tropospheric moisture strengthens as the middle and upper troposphere in the area with suppressed convection progressively experiences subsidence drying. In the center of the domain, on the other hand, the large-scale circulation further strengthens convection, which additionally moistens the middle and upper troposphere. The key point is that the large-scale temperature field homogenizes rapidly through the gravity-wave mechanism, whereas moisture relies on advection (both horizontal and vertical) to remove inhomogeneities, which is inefficient on large scales.

We purposely did not display the horizontal scale of the domain considered in Fig. 2, although the domain was much larger than the scale of a single cloud system. Development of the large-scale moisture gradient in the free troposphere involves the large-scale subsidence in the area with suppressed convection. Consequently, the time-scale for this process is much longer than the convective time scale as illustrated by the precipitable water plot in Fig. 1. The time scale of large-scale subsidence implies that the moisture-convection feedback is truly a large-scale phenomenon and it involves intraseasonal time scales (see section 2 in Grabowski and Moncrieff 2003 for details).

Strong coherence of MJO-like systems simulated in G03 suggests that the moisture-convection feedback operates very efficiently in the model that applies super-parameterization of convective processes. The same is also true when super-parameterization is applied in a real climate model as illustrated in Randall et al. (2003, Fig. 13). This seems to suggest that weak intraseasonal variability in traditional climate models is a result of weak sensitivity of traditional convective parameterizations to the free-tropospheric humidity as documented in Derbyshire et al. (2003). This point is further supported by simulations similar to those discussed in G03, but with the super-parameterization replaced by a traditional convective parameterization, the Emanuel scheme (Emanuel 1991). Results from these simulations are illustrated in Fig. 3.

As mentioned above, the free-tropospheric humidity impacts convective dynamics in two distinct ways. First, it affects the vertical cloud development due to impact of entrainment and buoyancy reversal on cloud dynamics. This effect cannot be captured in the Emanuel scheme because the subcloud air is always assumed to reach the level of neutral buoyancy for undiluted ascent. Second, free-tropospheric humidity affects the evaporation of rain falling outside clouds. This effect can be captured by the Emanuel scheme because a fraction of the precipitation that forms during undiluted ascent is assumed to feed unsaturated downdrafts outside clouds and is thus exposed to the environmental humidity. Unfortunately, in the standard configuration of the Emanuel scheme, the resulting sensitivity of the surface precipitation rate (hence the net heating in a column) to environmental humidity is weak (cf. Derbyshire et al. 2003). As illustrated in Fig. 3, the MJO-like coherence in the simulation applying the standard Emanuel scheme is much weaker when compared to CRCP simulations illustrated in Fig. 1.

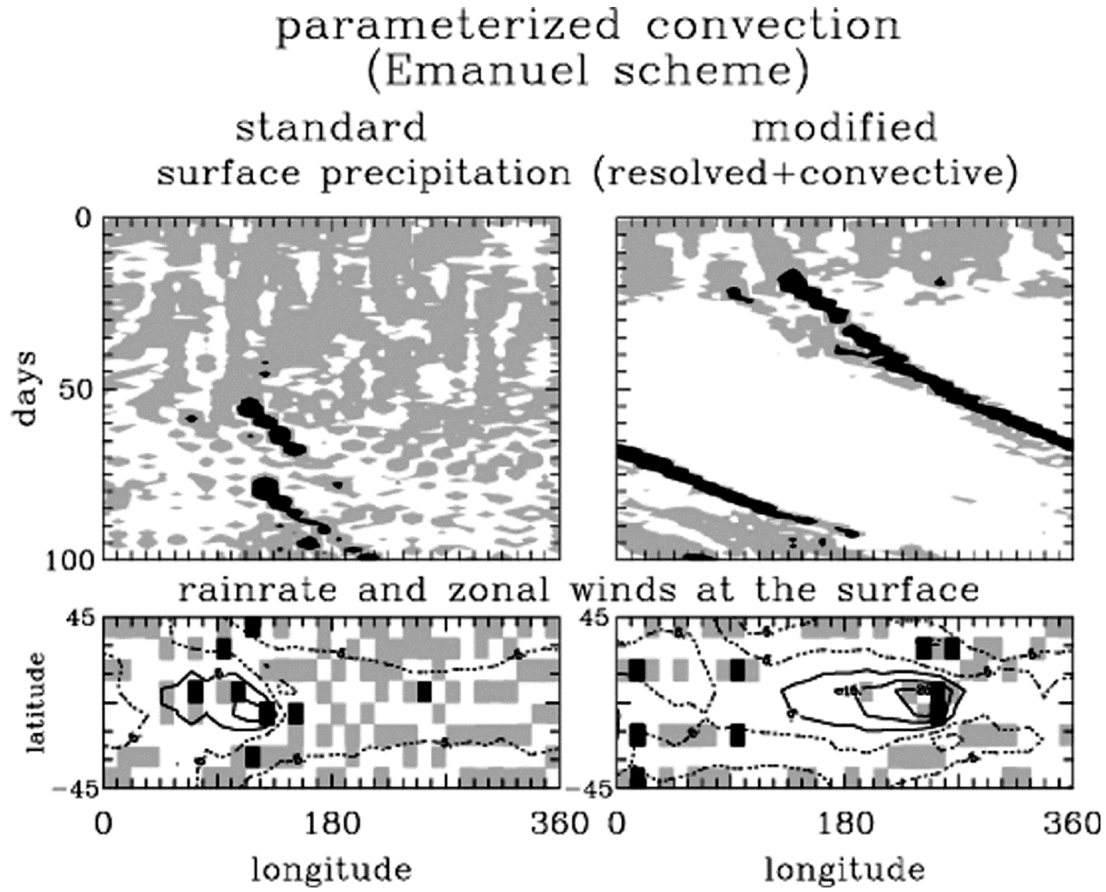

Figure 3. Results from the constant-SST aquaplanet simulation using Emanuel convective parameterization in its standard (left panels) and modified (right panels) configurations. Upper panels show Hovmöller diagrams of the surface precipitation at the equator. Lower panels show spatial distributions of surface precipitation and surface zonal winds at day 60 (left) and day 50 (right). Precipitation rate larger than 1.5 and 15 mm day^{-1} is shown using light and dark shading, respectively. Zonal winds are shown using solid and dashed contours for positive and negative values, respectively, with contour interval of 10 ms^{-1} starting from 5 ms^{-1}.

The sensitivity of the Emanuel scheme was artificially enhanced by increasing the amount of precipitation that falls outside clouds and is exposed to environmental humidity. In the modified Emanuel scheme applied in a simulation illustrated in Fig. 3, the amount of precipitation that falls outside clouds was increased from 0.12 to 0.30. This simple modification dramatically improves the simulated MJO-like coherence which develops after a mere 10 days and features surface precipitation and surface winds similar to the simulations applying the super-parameterization.

However, during the second half of the simulation using the modified Emanuel scheme, the MJO-like coherence is markedly distorted by the parameterized precipitation activated behind the leading-edge precipitation, i.e., within the westerly wind burst area. This region is characterized by strong vertical shear of the horizontal wind (i.e., strong westerlies at low levels and strong easterlies aloft). In the super-parameterization simulations deep convection seldom occurs there (e.g., Fig. 1, 3, and 5 in G03). This problem is particularly severe during the final 10 days of the simulation and compromises the coherence of the MJO-like system. This result points to another problem in convective parameterization: the convective scheme does not take into account the disruptive effect of environmental wind (e.g., vertical shear) on the development and evolution of convection.

Aquaplanet simulations using CRCP discussed in G03 and results applying Emanuel scheme discussed herein illustrate the role of moisture-convection feedback in intraseasonal oscillations in the tropics. They also point out, together with observational studies (e.g., Lin and Johnson 1996), to the role of various convective regimes within MJO systems (e.g., shallow versus deep, organized versus unorganized, etc). This aspect remains a major challenge for traditional convective parameterizations and it is likely the key for the MJO simulated by traditional climate models.

References

Derbyshire, S. H., I. Beau, P. Bechtold, J. Y. Grandpeix, J. M. Piriou, J. L. Redelsperger, and P. Soares, 2002: Sensitivity of moist convection to environmental humidity. *Quart. J. Roy. Met. Soc.; EUROCS Special Issue* (submitted).

Emanuel, K. A., 1991: A scheme for representing cumulus convection in large--scale models. *J. Atmos. Sci.*, **48**, 2313--2335.

Grabowski, W. W., 2001: Coupling cloud processes with the large-scale dynamics using the Cloud-Resolving Convection Parameterization (CRCP). *J. Atmos. Sci.*, **58**, 978-997.

Grabowski, W. W., 2003: MJO-like coherent structures: Sensitivity simulations using the Cloud-Resolving Convection Parameterization (CRCP). *J. Atmos. Sci.*, **60**, 847--864.

Grabowski, W. W., and M. W. Moncrieff, 2003: Moisture-convection feedback in the Tropics. *Quart. J. Roy. Met. Soc.; EUROCS Special Issue* (submitted).

Lin X., and R. H. Johnson, 1996: Kinematic and thermodynamic characteristics of the flow over the western pacific warm pool during TOGA COARE. *J. Atmos. Sci.*, **53**, 695-715.

Randall, D., M. Khairoutdinov, A. Arakawa, and W. Grabowski, 2003: Breaking the cloud-parameterization deadlock. *Bull. Amer. Meteor. Soc.* (in press).

Redelsperger, J.-L., D. B. Parsons, and F. Guichard, 2002: Recovery processes and factors limiting cloud-top height following the arrival of a dry intrusion observed during TOGA COARE. *J. Atmos. Sci.*, **59**, 2438-2457.

Tompkins, A. M., 2001: On the relationship between tropical convection and sea surface temperature. *J. Clim.*, **14**, 633-637.

Yanai, M., S. K. Esbensen, and J.-H. Chu, 1973: Determination of bulk properties of tropical cloud clusters from large-scale heat and moisture budgets. *J. Atmos. Sci.*, **30**, 611--627.